Conductivity and Photoconductivity of a p-type Organic Semiconductor under Ultra-Strong Coupling

Kalaivanan Nagarajan[#], Jino George[#], Anoop Thomas, Eloise Devaux, Thibault Chervy, Stefano Azzini, Aziz Jouaiti, Mir W. Hosseini, Anil Kumar, Cyriaque Genet and Thomas W. Ebbesen[*]

Dr. K. Nagarajan, Dr. J. George, Dr. A. Thomas, Dr. E. Devaux, Dr. T. Chervy, Dr. S. Azzini, Dr. C. Genet, Prof. T.W. Ebbesen
University of Strasbourg, CNRS, ISIS & icFRC, 8 allée G. Monge, 67000 Strasbourg, France
E-mail: ebbesen@unistra.fr

Dr. A. Jouaiti, Prof. M.W. Hosseini
University of Strasbourg, CNRS, Laboratoire de Tectonique Moléculaire & icFRC,
Institut Le Bel, 4 rue Blaise Pascal, 67070 Strasbourg Cedex, France

Prof. A. Kumar
Indian Institute of Technology Bombay, Department of Chemistry, Powai, Mumbai 400076, India
[#] These authors have contributed equally to this work.

Keywords: Strong coupling, organic semiconductors, conductivity, photoconductivity, p-type

Abstract: The conductivity and photoconductivity of the *p-type* semiconductor rr-P3HT was studied under light-matter strong coupling. The vacuum Rabi splitting with surface plasmon modes is ca. 1.2 eV corresponding to 54% of the transition energy. In this ultra-strong coupling regime, the conductivity is enhanced even for such *p-type* semiconductor demonstrating that ultra-strong coupling can modify the transport properties of the valence band. This effect is most easily explained by the finite photonic content of the polariton ground state under such extreme coupling conditions. Furthermore, the photoconductivity of rr-P3HT is also enhanced and show broadened spectral responses due to the formation of the hybrid polaritonic states. This is the first example of enhanced conductivity and photoconductivity for a *p-type* semiconductor under strong coupling. This illustrates yet again the potential of engineering the vacuum electromagnetic environment to improve the opto-electronic properties of materials.

During the last decade, it has been shown that light-matter strong coupling of organic materials can lead to modified and often improved properties which has stimulated considerable

interest in this topic.[1-35] For instance, it has been shown that charge transport can be enhanced by an order of magnitude in *n-type* semiconductors such as the perylene di-imide family of compounds and that the rate of energy transfer can be boosted, leading to nearly unit transfer efficiency.[15-22] Furthermore, energy transfer can even be achieved over distances well beyond what is expected from Förster theory.[21,22] These improved transport properties are the resultant of the delocalised character of the electronic excited state acquired through strong coupling. However, the role of hybrid light-matter states on the transport characteristics of *p-type* semiconductors, where valence band holes are the majority carriers are not yet understood, although it is also potentially important for organic electronics.[36-41] Interestingly, theory predicts that when excitons are coupled to a confined optical mode and one reaches the ultra-strong coupling regime, the ground state shifts to lower energies due to the large splitting of the first excited state and it acquires polaritonic character.[42] Such ground state shift has been confirmed experimentally.[43,44] The modification of magneto-transport properties, with a reduction in resistance, has recently been reported for ultra-strongly coupled 2D electron gas.[45] The fundamental question we explore here is whether the polaritonic character of the ground state leads to enhanced conductivity in *p-type* semiconductors since the valence band is modified.

Photoconductivity of organic materials could also benefit from the enhanced transport properties and the modified spectral response induced by the Rabi-splitting under strong coupling (Figure 1a). Since photoconductivity plays a fundamental role in many technological applications such as photodetectors, electrostatic imaging and photovoltaics,[46-52] we explore whether the photoconductivity can also be improved under strong coupling regime, another aspect that have not been addressed so far. For that purpose, we have studied a well-known *p-type* semiconductor, the regio-regular poly-(3-hexylthiophene) rr-P3HT whose structure is shown in Figure 1b and which was synthesized in our labs as described in the Methods section.

Light-matter strong coupling is achieved by placing a material with a well-defined transition in a resonant confined electromagnetic field such as a surface plasmon or a Fabry-Perot cavity mode. Under the right conditions, this strong interaction leads to the formation of two new hybrid light-matter states, known as polaritonic states P^+ and P^-, separated in energy by the Rabi-splitting $\hbar\Omega_R$ as illustrated in Figure 1a. In the absence of dissipation $\hbar\Omega_R$ is given by the following equation:1

$$\hbar\Omega_R = 2\sqrt{\frac{\hbar\omega}{2\varepsilon_0 V}}\,.\,d\,\times\sqrt{n_{ph}+1} \qquad (1)$$

where ε_0 is the permittivity of free space, V the volume of the confined mode, d the transition dipole moment of the material and n_{ph} is the number of photons in the system. It can be immediately seen from equation (1) that the strong coupling can occur even when n_{ph} goes to zero, implying that even in the dark the Rabi splitting has a finite value. This is due to the coupling with the zero-point fluctuations of the electromagnetic mode (*i.e.* the vacuum field). Furthermore it can be shown that the Rabi-splitting is enhanced by placing a large number N of oscillators or molecules in the confined field of a single mode. In this ensemble coupling where $\hbar\Omega_R \propto \sqrt{N}$, there are large number of possible combinations resulting in the formation of dark states (DS) along with the bright P^+ and P^- states (Figure 1a). Besides the formation of polaritonic states in the excitation spectrum of strongly coupled systems, the ground state can also be affected for large enough coupling strength through anti-resonant coupling to the double excitation manifold (equation (1) was derived in the rotating-wave approximation). As discussed above, a detailed analysis of this ultra-strong coupling regime[42] predicts a ground state shift that increases with increasing Rabi-splitting in agreement with more recent experiments.[43,44]

The conductivity and the photoconductivity of the rr-P3HT were studied on Ag nano-hole arrays between drain and source electrodes, using the same approach as in ref. 15. Ag was chosen for its capacity to sustain low-loss surface plasmon modes in the wavelength range of interest while still providing good injection capacity for the electrical measurements.[15,37] As detailed in the Experimental section, the hexagonal hole arrays were milled with a Zeiss Auriga dual beam FIB/SEM and the period p of the holes were varied in such a way that the plasmonic resonances are in the same range as the first absorption bands of the semiconductors (see Figure 1c). The compound was spin-coated on the hole arrays (ca. 85 nm thick films) and first, the strong coupling regime was verified by measuring their transmission spectra and comparing them with the bare hole arrays (Figure 1d). The Rabi splitting are estimated to be ca. 1.2 eV for rr-P3HT corresponding to 54% of the transition energy as explained in the Supporting Information. Such large Rabi-splitting indicate that the system is in the ultra-strong coupling regime where all the states of the system are modified with significant consequences as we will discuss further down. It should be noted that it is hard to estimate the Rabi splitting from the spectra of hole arrays due to overlapping surface plasmon modes, as discussed elsewhere.[9] We

therefore double checked the splitting induced for the same films coupled to the first mode of Fabry-Perot cavities (see Supporting Information, Figure S1) which are known to give roughly the same values.[9] Note that the dispersion curves in the ultra-strong regime are very flat due to the emergence of a polaritonic band gap in the resonance region as reported and discussed in detail in ref. 53.

We then measured the I-V (current-voltage) curves of the various samples as a function of the hole period over a small voltage range (-0.5 to 0.5 V) shown in Figure 2 (a) and (b), in the configuration explained in the Supporting Information. Because we analyze the current over such small voltage range, the I-V curves are linear but over larger voltages they are non-linear as expected for a semiconductor. Figure 2 (c) and (d) replots the current data at ± 0.5V as a function of $2\pi/p$ for both the dark current and the photocurrent of rr-P3HT coated hole arrays. Interestingly, both the dark current (Figure 2 (c)) and the photocurrent (Figure 2 (d)) vary in similar way although the absolute values are higher under illumination. A sharp peak appears in both measurements when the absorption peak of rr-P3HT absorption crosses the (1,1) mode of the hexagonal plasmonic array (blue curve in Figure 2 (e)) and undergoes ultra-strong coupling. Since varying the periodicity of the hole array leads to on- and off-resonance conditions with respect to the absorption of rr-P3HT, the plots in Figure 2(c) and (d) shows how the current varies when the system goes in and out of strong coupling. Interestingly, the photoconductivity benefits from the enhanced conductivity in the same way as the dark current does under strong coupling. When compared to the conductivity on a flat metal surface, the enhancement is a factor of 8 for the dark current and 6 for the photocurrent. These enhancements are slightly smaller than those observed for *n-type* perylene di-imide semiconductor in our earlier study which most likely relates to the level of order in the organic film which plays an important role as we demonstrated earlier.[15] It should be noted that oxygen can modify the conductivity of rr-P3HT compounds. However we checked that the results for our coated samples were the same within experimental error under nitrogen atmosphere. It was also verified that the observed boosts in current where not due to artifacts such as the cuts that are made in the hole arrays. First of all, we have tested various different organic semiconductors and nevertheless the enhanced conductivity, if it occurs, is always at strong coupling although this happens for different periods. Secondly, as shown in the SEM image of the array after the cutting (Figure S3), the edged is smoothed by the FIB. Thirdly, we always test a random hole array which has no pronounced mode and it displays no enhancement (see Figure S4). Finally, the flat metal film is electrically floating and with the Shottky barrier at the interface with the semiconductor, it does not contribute to the conductivity.

This is the first example of enhanced conductivity for a *p-type* semiconductor under strong coupling which indicates that the charge carrying valence band is also affected by the formation of polaritonic states. As mentioned earlier, the system is in the ultra-strong coupling regime under the collective coupling conditions where counter-rotating terms and depolarization shifts cannot be neglected, leading to major changes in all the other eigenstates through configuration interaction. This leads to a finite admixture of virtual photons in the ground-state of the system, in our case the ground state where hole transport occurs.[42,54,55] With the method described in the Supporting Information, we estimate this photonic content to be on the order of 1% for the ground state or valence band of rr-P3HT. In other words, the ground state is then further delocalized by the polaritonic character induced by the ultra-strong coupling. This is the most likely explanation of the enhanced conductivity as compared to the bare *p-type* polymer. It may appear surprising that such a low photonic fraction in the ground state can affect to such an extent the conductivity of the material. One should however be cautious in comparing the ground state photonic fraction to the excited state photonic fraction quoted in our previous work on *n-type* semiconductors.[15] Indeed, the competing energy pathways and dynamics are much different in those two cases and this fact does not allow for a simple proportionality argument. In particular, we cannot assume that the effect of 1% photonic content in the ground state for *p-type* transport would be smaller than the effect of 50% photonic fraction in the excited state for a *n-type* charge carrier. It should also be noted that the ground state photonic fraction reached in our system compares with that obtained in state-of-the-art experiments carried on different ultra-strong coupling platforms.[45, 54-57] Although the system is very different, modifications of the magneto-transport measurements in a 2D electron gas coupled to a THz resonator was recently reported, another demonstration of the impact of ultra-strong coupling on the ground-state properties of the host material.[45]

We now turn to the photoconductivity measurements. Figure 3 (a) shows the linear dependence of the photocurrent on the excitation intensity for rr-P3HT when measured under white light cw (continuous wave) illumination. At such low intensities per unit area (<15 mW per cm^2), the fraction of excited state absorbers remains at all time negligible and as a consequence there is no significant depopulation of the ground state and the collective Rabi splitting is unmodified. From Eq. (1), one might expect that the Rabi splitting is increased under illumination. However the dependence on the number of photons has only been derived in the limit of a single absorber and no effect of the illumination has ever been reported for collective coupling as in these experiments. The quantum yield for the photogeneration of charge carriers is estimated to be ca. 5×10^{-3} for rr-P3HT (520 nm illumination). The spectral response of the

photocurrent was also studied using a tunable pulsed laser source (NKT laser) under strong coupling conditions and compared to that of the bare film. The ratio of the current for these two conditions is shown in Figure 3 (b) and reveals enhanced photocurrent at longer wavelengths than the absorbance peak of the bare rr-P3HT with a maximum around 620 nm. This corresponds to the P- peak. Since the spectral enhancement at long wavelengths is due to the Rabi splitting, a similar enhancement is expected to be seen at shorter wavelength corresponding to the P+ transition but our tunable laser system cannot reach the corresponding wavelengths.

For purposes of comparison, we also studied the photoconductivity of a perylene di-imide (PDI) *n-type* semiconductor under strong coupling. We already shown that this class of compounds gives rise the enhanced conductivity in ref. 15. The compound is a slightly different derivative whose structure is shown in the Supporting Information. Figure 4 summarizes the results. Comparing panels (a) and (b), we observe that the photoconductivity of PDI is also enhanced upon ultra-strong coupling (Rabi splitting is 34% of transition energy, see Supporting Information) since two current peaks appear at the crossing of the PDI film absorbance peak and the plasmonic modes. Figure 4 (c) shows the linear dependence of the current with illumination power and Figure 4 (d) shows that just as for rr-P3HT, the spectral response is enhanced where P- absorbs.

In conclusion, using a *p-type* organic semiconductor, we have demonstrated for the first time that hole transport in the ground state can also be enhanced by strong coupling. This is in turn a direct evidence of the polaritonic character of the valence band. We have also shown that the photoconductivity, like conductivity, can be boosted by the formation of extended polaritonic states and in addition their spectral response can be extended and tailored by the coupling strength. This works for both *n-* and *p-type* semiconductors. This proof-of-principle study opens the door for more detailed analysis of photoconductivity by time resolved pump-probe techniques which will provide insight into the dynamics of charge carriers in the strong and ultra-strong coupling regimes. Strong coupling is easy to implement in a variety of configurations. We therefore expect that such results will find applications in devices where photoconductivity plays a role, in particular in photovoltaics and photodetectors. More broadly speaking, taken together with other investigations, it shows the potential of engineering the electromagnetic vacuum environment for material science and devices.

Experimental Section

Synthesis of materials:

Regioregular poly(3-hexylthiophene), rr-P3HT was synthesized and purified as reported earlier.[58]

Two-terminal device with nanohole arrays for photoconductivity measurements.

All the 2-terminal electrodes were realized on a glass substrate BK7 (25×25 mm) after standard cleaning procedures with Hellmanex™ III solution (Sigma Aldrich; 1.0% solution in milliQ water) in a 35 kHz sonication bath, then rinsed with water and sonicated for 1 h in (spectroscopically pure) ethanol. The glass substrates were then dried in an oven covered with Aluminium foil. Ag electrodes (100 nm) were fabricated using a metallic cross mask containing 12 fingers (approx. 50 µm width) in an electron beam evaporator (Plassys ME 300) at optimized working pressure (~10^{-6} mbar) and deposition rates (~2 nm s^{-1}). Plasmonic hole arrays were generated by the NPVE software program and milled using a Carl Zeiss Auriga FIB system. 1.0 wt% of PDI and rr-P3HT solutions were freshly prepared by dissolving the molecules in spectroscopic grade anhydrous chloroform and trichloroethylene respectively at ambient conditions and spin-coating onto the electrodes at 1000 r.p.m., to achieve 85 nm-thick films. The reddish, smooth PDI and rr-P3HT thin-films were completely dried and annealed on a hot plate above the glass transition temperature. A passive layer of PVA was spin-coated (~500 nm) further to protect the active layer to avoid direct exposure to air and moisture.

The electrical characterization of the 2-terminal device was carried out by means of a Cascade Microtech MPS-150 probe station equipped with micro-positioners to contact the electrode pads. Both the dark current and photoconductivity I–V characteristics are recorded by means of a Keithley 2636B source meter interfaced with Labtracer 2.0 software. Photo-current generation was tested under white light cw illumination and with a super-continuum ps pulsed laser (NKT Photonics) with a nominal power of 100 mW to 200 mW, with variable wavelength (500-800 nm; 10 nm FWHM) provided by a SuperK tunable single line filter. The output of the FC/PC fibre was directed to the centre of the electrode covering a spot size of 2 mm in diameter.

Supporting Information

Supporting Information is available from the Wiley Online Library or from the author.

Acknowledgments

We acknowledge support of the International Center for Frontier Research in Chemistry (icFRC, Strasbourg), the ANR Equipex Union (ANR-10-EQPX-52-01), the Labex NIE projects (ANR-11-LABX-0058 NIE) and CSC (ANR-10-LABX- 0026 CSC) within the Investissement d'Avenir program ANR-10-IDEX-0002-02.

References

[1] T. W. Ebbesen, *Acc. Chem. Res.* **2016**, *49*, 2403.
[2] P. Törmä, W. L. Barnes, *Rep. Prog. Phys.* **2015**, *78*, 013901.
[3] S. Kéna-Cohen, S. R. Forrest, *Nat. Photonics* **2010**, *4*, 371.
[4] D. Ballarini, M. De Giorgi, E. Cancellieri, R. Houdré, E. Giacobino, R. Cingolani, A. Bramati, G. Gigli, D. Sanvitto, *Nat. Commun.* **2013**, *4*, 1778.
[5] J. D. Plumhof, T. Stöferle, L. Mai, U. Scherf, R. F. Mahrt, *Nat. Mater.* **2013**, *13*, 247.
[6] T. Chervy, J. Xu, Y. Duan, C. Wang, L. Mager, M. Frerejean, J. A. W. Münninghoff, P. Tinnemans, J. A. Hutchison, C. Genet, A. E. Rowan, T. Rasing, T. W. Ebbesen, *Nano Lett.* **2016**, *16*, 7352.
[7] S. Aberra Guebrou, C. Symonds, E. Homeyer, J. C. Plenet, Y. N. Gartstein, V. M. Agranovich, J. Bellessa, *Phys. Rev. Lett.* **2012**, *108*, 066401.
[8] L. Shi, T. K. Hakala, H. T. Rekola, J. P. Martikainen, R. J. Moerland, P. Törmä, *Phys. Rev. Lett.* **2014**, *112*, 153002.
[9] T. Schwartz, J. A. Hutchison, C. Genet, T. W. Ebbesen, *Phys. Rev. Lett.* **2011**, *106*, 196405.
[10] J. A. Hutchison, S. Tal, G. Cyriaque, D. Eloïse, T. W. Ebbesen, *Angew. Chem. Int. Ed.* **2012,** *51*, 1592.
[11] J. A. Hutchison, A. Liscio, T. Schwartz, A. Canaguier-Durand, C. Genet, V. Palermo, P. Samori, T.W. Ebbesen, *Adv. Mater.* **2013**, *25*, 2481.
[12] S. Wang, A. Mika, J. A. Hutchison, C. Genet, A. Jouaiti, M. W. Hosseini, T. W. Ebbesen, *Nanoscale* **2014**, *6*, 7243.
[13] S. Wang, T. Chervy, J. George, J. A. Hutchison, C. Genet, T. W. Ebbesen, *J. Phys. Chem. Lett.* **2014**, *5*, 1433.
[14] A. Shalabney, J. George, J. Hutchison, G. Pupillo, C. Genet, T. W. Ebbesen, *Nat. Commun.* **2015**, *6*, 5981.
[15] E. Orgiu, J. George, J. A. Hutchison, E. Devaux, J. F. Dayen, B. Doudin, F. Stellacci, C. Genet, J. Schachenmayer, C. Genes, G. Pupillo, P. Samorì, T. W. Ebbesen, *Nat. Mater.* **2015**, *14*, 1123.
[16] D. Hagenmüller, J. Schachenmayer, S. Schütz, C. Genes, G. Pupillo, *Phys. Rev. Lett.* **2017**, *119*, 223601.
[17] Z. Xiaolan, C. Thibault, W. Shaojun, G. Jino, T. Anoop, J. A. Hutchison, D. Eloise, G. Cyriaque, T. W. Ebbesen, *Angew. Chem. Int. Ed.* **2016**, *55*, 6202.
[18] J. Feist, F. J. Garcia-Vidal, *Phys. Rev. Lett.* **2015**, *114*, 196402.

[19] J. Schachenmayer, C. Genes, E. Tignone, G. Pupillo, *Phys. Rev. Lett.* **2015**, *114*, 196403.
[20] D. M. Coles, N. Somaschi, P. Michetti, C. Clark, P. G. Lagoudakis, P. G. Savvidis, D. G. Lidzey, *Nat. Mater.* **2014**, *13*, 712.
[21] C. Gonzalez-Ballestero, J. Feist, E. Moreno, F. J. Garcia-Vidal, *Phys. Rev. B* **2015**, *92*, 121402.
[22] X. Zhong, T. Chervy, L. Zhang, A. Thomas, J. George, C. Genet, J. A. Hutchison, T. W. Ebbesen, *Angew. Chem. Int. Ed.* **2017**, *56*, 9034.
[23] A. Thomas, J. George, A. Shalabney, M. Dryzhakov, S. J. Varma, J. Moran, T. Chervy, X. Zhong, E. Devaux, C. Genet, J. A. Hutchison, T. W. Ebbesen, *Angew. Chem. Int. Ed.* **2016**, *55*, 11462.
[24] P. Vasa, W. Wang, R. Pomraenke, M. Lammers, M. Maiuri, C. Manzoni, G. Cerullo, C. Lienau, *Nat. Photonics* **2013**, *7*, 128.
[25] G. Zengin, M. Wersäll, S. Nilsson, T. J. Antosiewicz, M. Käll, T. Shegai, *Phys. Rev. Lett.* **2015**, *114*, 157401.
[26] A. Berrier, R. Cools, C. Arnold, P. Offermans, M. Crego-Calama, S. H. Brongersma, J. Gómez-Rivas, *ACS Nano* **2011**, *5*, 6226.
[27] J. Li, K. Ueno, H. Uehara, J. Guo, T. Oshikiri, H. Misawa, *J. Phys. Chem. Lett.* **2016**, *7*, 2786.
[28] I. Carmeli, M. Cohen, O. Heifler, Y. Lilach, Z. Zalevsky, V. Mujica, S. Richter, *Nat. Commun.* **2015**, *6*, 7334.
[29] J. A. Ćwik, P. Kirton, S. De Liberato, J. Keeling, *Phys. Rev. A.* **2016**, *93*, 033840.
[30] F. Herrera, F. C. Spano, *Phys. Rev. Lett.* **2016**, *116*, 238301.
[31] C. Pellegrini, J. Flick, I. V. Tokatly, H. Appel, A. Rubio, *Phys. Rev. Lett.* **2015**, *115*, 093001.
[32] G. G. Rozenman, K. Akulov, A. Golombek, T. Schwartz, *ACS Photonics* **2018**, *5*, 105.
[33] H. L. Luk, J. Feist, J. J. Toppari, G. Groenhof, *J. Chem. Theory Comput.* **2017**, *13*, 4324.
[34] M. Cirio, S. De Liberato, N. Lambert, F. Nori, *Phys. Rev. Lett.* **2016**, *116*, 113601.
[35] K. Stranius, M. Hertzog, K. Börjesson, *Nat. Commun.* **2018**, *9*, 2273.
[36] O. G. Jesus, S. Alberto, *Adv. Funct. Mater.* **2017**, *27*, 1701791.
[37] H. Yan, Z. Chen, Y. Zheng, C. Newman, J. R. Quinn, F. Dötz, M. Kastler, A. Facchetti, *Nature* **2009**, *457*, 679.
[38] S. R. Forrest, *Nature* **2004**, *428*, 911.
[39] A.C. Arias , J.D. Mackenzie, I. McCulloch, J. Rivnay, A. Salleo, *Chem. Rev.* **2010**, *110*, 3.
[40] S. Himmelberger, A. Salleo, *MRS Commun*. **2015**, *5*, 383.
[41] A. Salleo, *Nature Mat.* **2014**, *14*, 1077.
[42] C. Ciuti, G. Bastard, I. Carusotto, *Phys. Rev. B* **2005**, *72*, 115303.
[43] P. Forn-Díaz, J. Lisenfeld, D. Marcos, J. J. García-Ripoll, E. Solano, C. J. P. M. Harmans, J. E. Mooij, *Phys. Rev. Lett.* **2010**, *105*, 237001.
[44] A. Canaguier-Durand, E. Devaux, J. George, Y. Pang, J. A. Hutchison, T. Schwartz, C. Genet, N. Wilhelms, J.M. Lehn, T. W. Ebbesen, *Angew. Chem. Int. Ed.* **2013**, *52*, 10533.

[45] G. L. Paravicini-Bagliani, F. Appugliese, E. Richter, F. Valmorra, J. Keller, M. Beck, C. Rossler, T. Ihn, K. Ensslin, G. Scalari, J. Faist, *Nature Physics* **2018,** https://doi.org/10.1038/s41567-018-0346-y
[46] Y. Wang, *Nature* **1992**, *356*, 585.
[47] Y. Yasutani, A. Saeki, T. Fukumatsu, Y. Koizumi, S. Seki, *Chem. Lett.* **2013**, *42*, 19.
[48] H. Najafov, B. Lee, Q. Zhou, L. C. Feldman, V. Podzorov, *Nat. Mater.* **2010**, *9*, 938.
[49] G. A. O'Brien, A. J. Quinn, D. A. Tanner, G. Redmond, *Adv. Mater.* **2006**, *18*, 2379.
[50] P. Irkhin, H. Najafov, V. Podzorov, *Sci. Rep.* **2015**, *5*, 15323.
[51] Z. Huang, W. Zhou, J. Huang, J. Wu, Y. Gao, Y. Qu, J. Chu, *Sci. Rep.* **2016**, *6*, 22938.
[52] J. J. Walsh, J. R. Lee, E. R. Draper, S. M. King, F. Jäckel, M. A. Zwijnenburg, D. J. Adams, A. J. Cowan, *J. Phys. Chem. C* **2016**, *120*, 18479.
[53] J. George, T. Chervy, A. Shalabney, E. Devaux, H. Hiura, C. Genet, T. W. Ebbesen, *Phys. Rev. Lett.* **2016**, *117*, 153601.
[54] Y. Todorov, A. M. Andrews, R. Colombelli, S. De Liberato, C. Ciuti, P. Klang, G. Strasser, C. Sirtori, *Phys. Rev. Lett.* **2010**, *105*, 196402.
[55] G. Scalari, C. Maissen, D. Turčinková, D. Hagenmüller, S. De Liberato, C. Ciuti, C. Reichl, D. Schuh, W. Wegscheider, M. Beck, J. Faist, *Science* **2012**, *335*, 1323.
[56] B. Askenazi, A. Vasanelli, A. Delteil, Y. Todorov, L. C. Andreani, G. Beaudoin, I. Sagnes, C. Sirtori, *New. J. Phys.* **2014**, *16*, 043029.
[57] S. Gambino, M. Mazzeo, A. Genco, O. Di Stefano, S. Savasta, S. Patanè, D. Ballarini, F. Mangione, G. Lerario, D. Sanvitto, G. Gigli, *ACS Photonics* **2014**, *1*, 1042.
[58] A. Nawaz, M. S. Meruvia, D. L. Tarange, S. P. Gopinathan, A. Kumar, A. Kumar, H. Bhunia, A. J. Pal, I. A. Hümmelgen, *Org. Electron.* **2016**, *38*, 89.

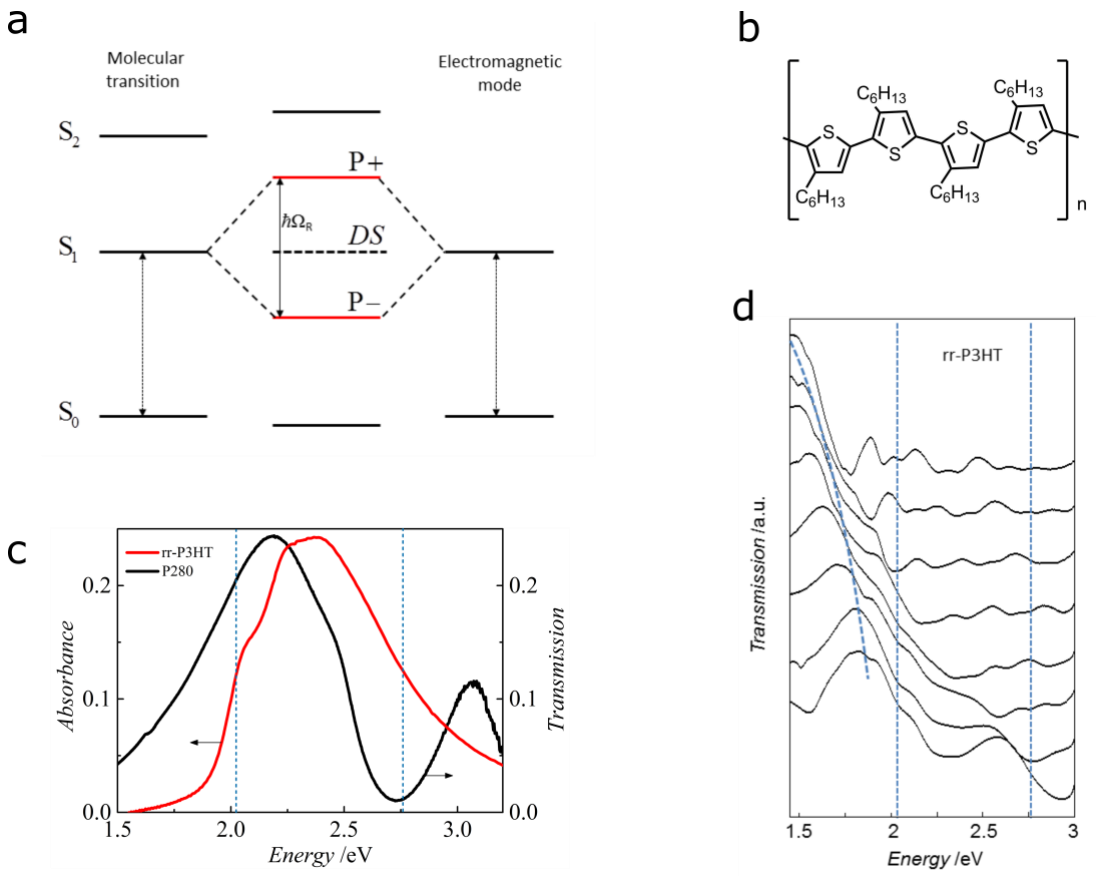

Figure 1. (a) Illustration of strong coupling between a molecular electronic transition and a resonant electromagnetic mode. Two hybrid light-matter states P+ and P- are formed, separated by a Rabi splitting energy $\hbar\Omega_R$. Dark states (DS) are also formed from the collective coupling process. (b) Molecular structure of the *p-type* semiconductor rr-P3HT polymer. (c) Absorbance spectra of a thin film of rr-P3HT (red line) and the transmission spectrum of a hexagonal hole array in Ag with a period of 280 nm (black line) displaying two surface plasmon modes. (d) Normal incidence transmission spectra of the surface plasmon resonances of hexagonal hole arrays in a Ag film coated with 85 nm thick film of rr-P3HT obtained for different periods between 240 nm and 520 nm every 40 nm. The dashed vertical lines indicate the position of the full width half maximum of the absorbance of rr-P3HT. The dashed curved line is a guide to the eye.

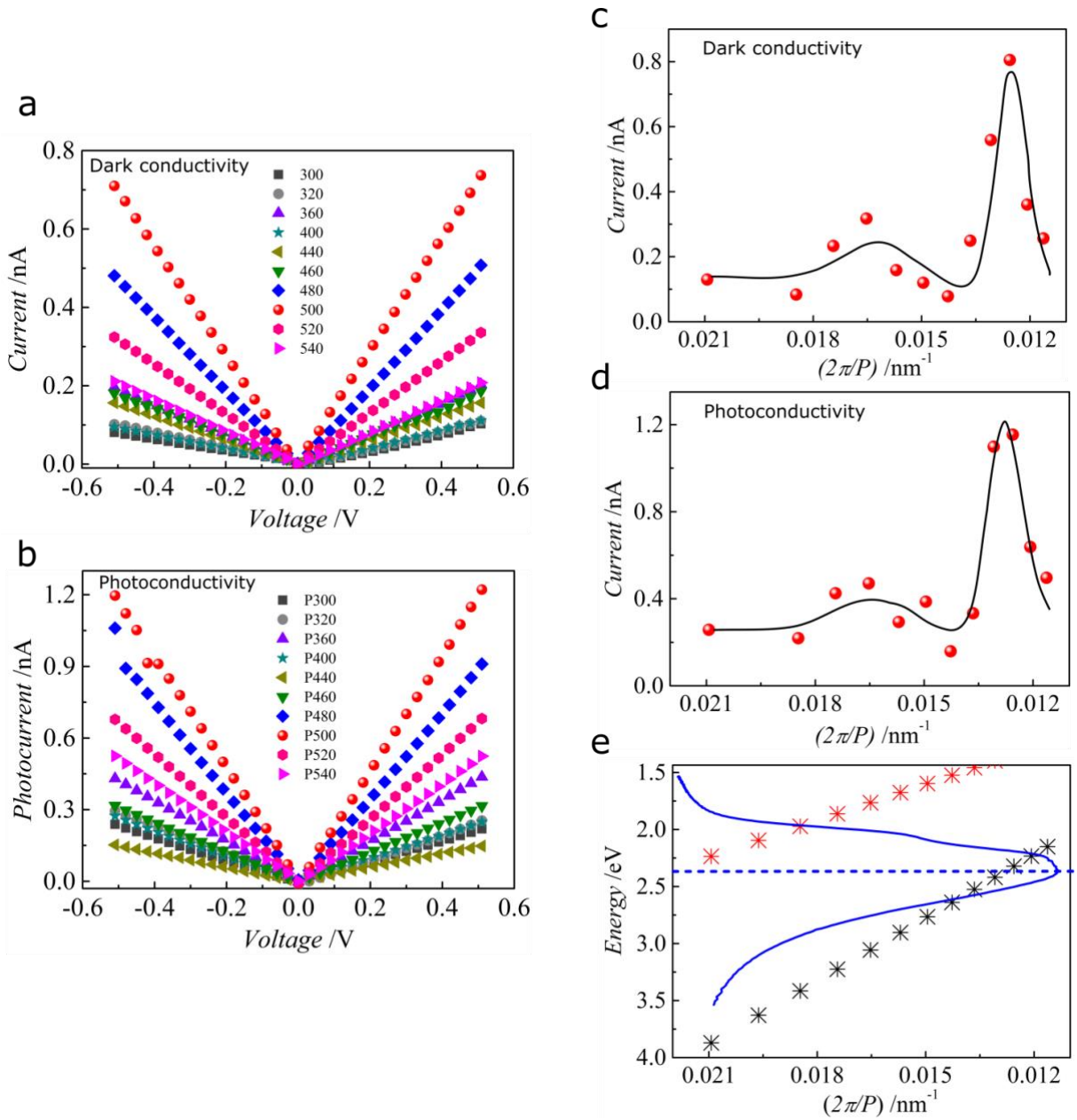

Figure 2. (a) Current-voltage (I-V) curves of the rr-P3HT samples as a function of the period P of the hole arrays. (b) Idem under illumination at 520 nm (47 mW cm^{-2}). (c) Current (red dots) measured at ± 0.5 V as a function $2\pi/p$ where p is the period of the hexagonal plasmonic array on which the rr-P3HT is spin-coated. (d), idem under illumination at 520 nm (47 mW cm^{-2}). (e) The resonance in the current in (c) and (d) corresponds to the intersection of the molecular absorbance (blue solid line with maxima indicated by dashed line) and the (1,1) mode (black stars) of the Ag array plasmon resonances where strong coupling occurs. The (1,0) mode of the hole array is indicated by red stars.

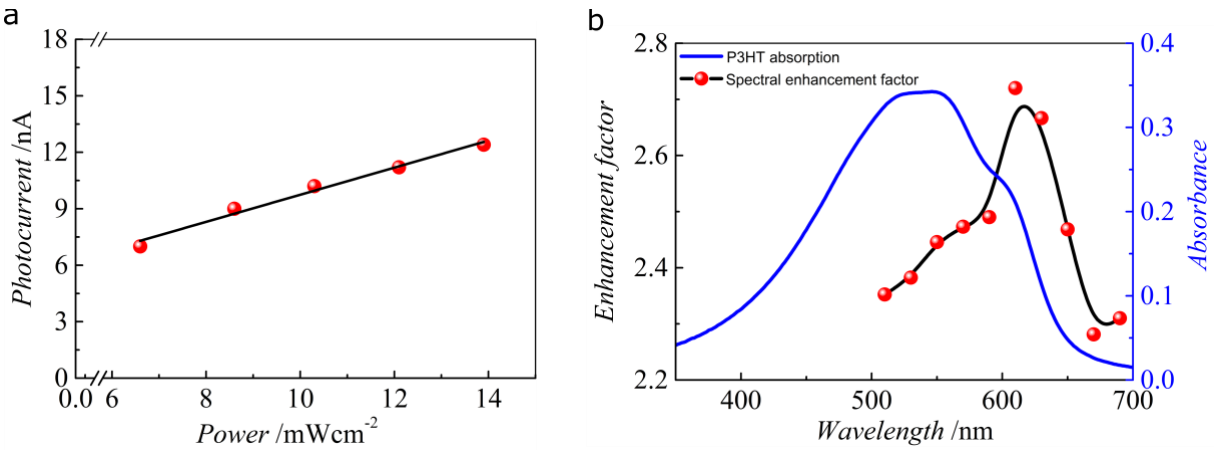

Figure 3. (a) Photocurrent as function of the white light illumination power for rr-P3HT under strong coupling (P= 500 nm). (b) Spectral response under ultra-strong coupling (red dots, P=500 nm)) as a function of excitation wavelength, the enhancement factor is the ratio of the photocurrent divided by the corresponding photocurrent of an uncoupled rr-P3HT film. A tunable pulsed laser with a 10 nm bandpass was used for this study. The peak at 620 nm corresponds to the P- peak. The blue curve gives the absorbance spectrum of the bare rr-P3HT film. The black lines are guides to the eye.

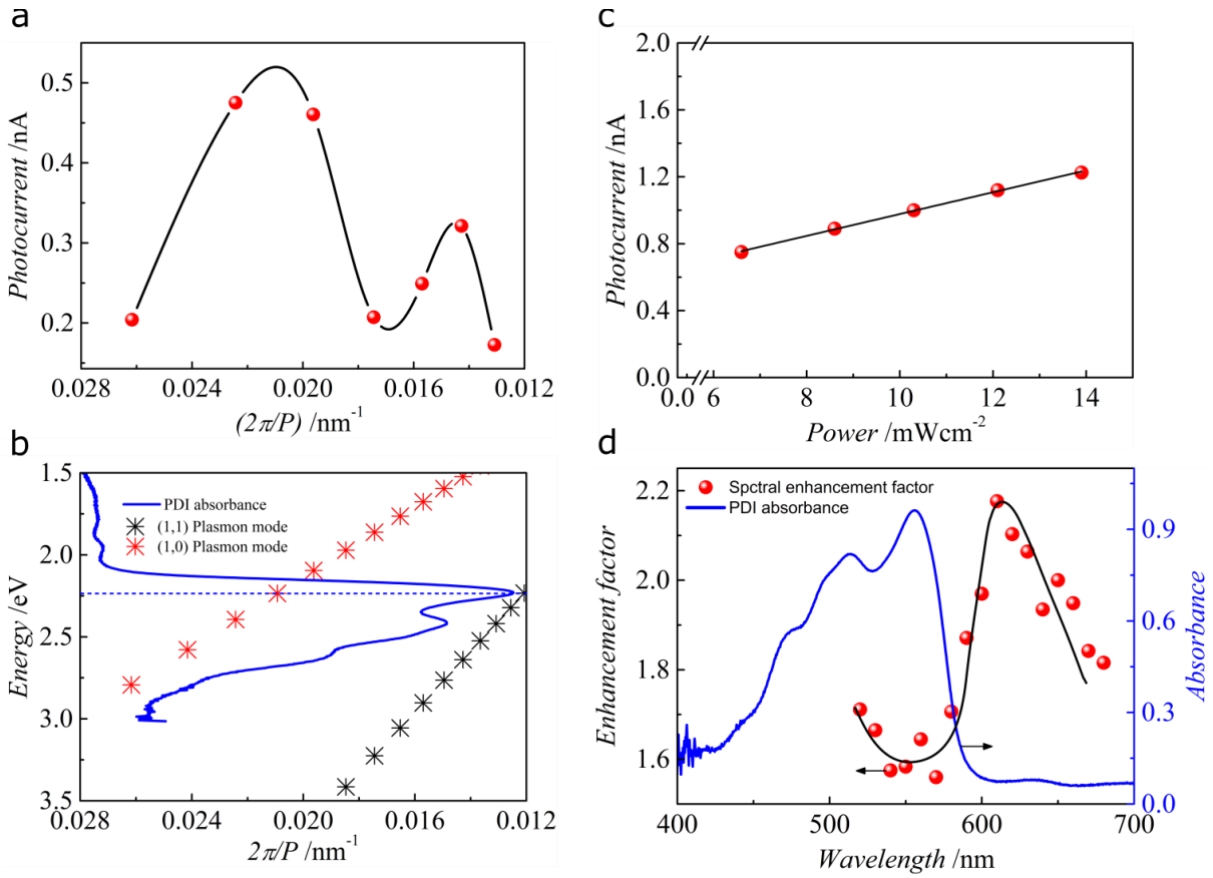

Figure 4. (a) Photocurrent (red dots) under illumination at 570 nm (41 mW cm^{-2}) measured at ± 0.5 V as a function $2\pi/p$ where p is the period of the hexagonal plasmonic array on which the *n-type* semiconductor PDI has been spin-coated. (b) The two resonances in the current in (a) correspond to the intersection of the PDI absorbance (blue solid curve with maximum indicated by dashed line) and the (1,0) (red stars) and (1,1) (black stars) modes of the Ag array plasmon resonances. At these intersections strong coupling occurs. (c) Photocurrent as function of the white light illumination power for PDI under strong coupling (P=440 nm). (d) Spectral response under ultra-strong coupling (red dots, P=440 nm) as a function of excitation wavelength, the enhancement factor is the ratio of the photocurrent divided by the corresponding photocurrent of an uncoupled PDI film. A tunable pulsed laser with a 10 nm bandpass was used for this study. The broad peak between 600 and 650 nm corresponds to the P- peak. The blue curve gives the absorbance spectrum of the bare PDI film. The black lines are guides to the eye.